



Sandstone reservoir zonation of the north-western Bredasdorp Basin South Africa using core data

Mimonitu Opuwari^{*}, Nehemiah Dominick

Petroleum Geosciences Research Group, Department of Earth Sciences, University of the Western Cape, Cape Town, South Africa

ARTICLE INFO

Keywords:

Pore throat radius
Flow capacity
Flow zone indicator
Bredasdorp Basin
Stratigraphy modified Lorentz Plot

ABSTRACT

This study delineates sandstone reservoir flow zones in the north-western Bredasdorp Basin, offshore South Africa, using conventional core porosity and permeability data. The workflow begins by integrating sedimentology reports and logs to identify lithofacies before evaluating petrophysical flow zones. Three lithofacies were classified as lithofacies 1, 2, and 3. Lithofacies 1 is a silty shale and bioturbated sandstone, lithofacies 2 is an interbedded sandstone and shale, with very fine sandstone with well-sorted grains, and is heavily cemented. Conversely, lithofacies 3 is a fine-to medium-grained sandstone with minor shale that is moderately cementation. Lithofacies 3 is ranked as the best reservoir rock, followed by lithofacies 2 and 1.

Four independent reservoir zonation methods (permeability anisotropy, Winland r35 pore throat, flow zone indicator (FZI), and stratigraphic modified Lorenz lot (SMLP)) were applied to core samples from three wells (MO4, MO5, and MO6). The core samples predominantly had slight anisotropic permeability (0.5–1.1). The reservoir units were ranked into four flow zone categories as tight, very low, low, and moderate, based on porosity and permeability, and calculated parameters. Owing to the reservoir unit heterogeneity, the classification was based on average values. The moderate zone exhibits the best reservoir quality, which is associated with lithofacies 3. The very-low flow zone extends laterally to all wells. The tight zones showed fluid storage potential but no flow capacity. In general, the lithofacies do not always correspond to petrophysical flow zones. The moderate and low flow zones identified in well MO5 are comparable to previously identified flow zones (MO2, MO3, and MO1) in the Western Bredasdorp Basin.

1. Introduction

Petrophysical rock zonation is defined as the classification of rocks into separate zones based on their static and dynamic behaviour (Gomes et al., 2008; Khalid et al., 2020; Porras and Campos, 2001; Opuwari, 2010), which is a function of their geological and petrophysical properties. Typically, rocks classified together would have been deposited under similar conditions and subjected to similar diagenetic processes. Grouping reservoirs into distinct zones is achieved based on the connection between permeability and porosity (Carman, 1937). The hydraulic flow unit (HFU) and flow unit (FU) help classify and account for the influence of rock type on a reservoir's fluid flow. The FU was defined as a bulk reservoir rock in which petrophysical and geological properties affecting flow are consistent and probably unique from the properties of surrounding rock volumes (Hearn et al., 1984; Ebanks, 1987). The HFU is identified as a reservoir rock section with unique fluid flow characteristics at the pore scale based on similarities in

petrophysical parameters (Amaefule et al., 1993; Mahjour et al., 2016). Diverse quantitative approaches exist to describe reservoir rocks and their petrophysical properties using empirical calculations from flow zone indicators (FZIs) (Amaefule et al., 1993; Kassab et al., 2015; El Sharawy and Nabawy, 2016; Nabawy and Barakat, 2017; Nabawy et al., 2018).

Rock typing, petrophysical flow zonation, and FU detection are more challenging in clastic reservoirs with a uniform pore system. However, such challenges are addressed through an integrated reservoir workflow that involves different techniques and datasets (Khadem et al., 2020). An appropriate application of the flow zonation method will result in an accurate permeability estimation, unique permeability–porosity relationship, and more realistic simulation outcomes (Al-Jawad and Saleh, 2020; Khadem et al., 2020; Nabawy and Al-Azazi, 2015; M. Opuwari et al., 2020a; Opuwari et al., 2019; Shalaby, 2021).

Stratigraphic modified Lorenz plots (SMLPs), which involve the graphical integration of geological frameworks, pore types, flow

^{*} Corresponding author.

E-mail addresses: mopuwari@uwc.ac.za (M. Opuwari), 2707130@myuwc.ac.za (N. Dominick).

capacities, and storage values, are used to define FUs in reservoir rocks (Gomes et al., 2008; Gunter et al., 1997; Slatt and Hopkins, 1990; Tiab and Donaldson, 2015). To better understand the reservoir rocks within the Bredasdorp Basin, core samples were characterised to construct SMLPs and determine the FZIs, HFUs, and FUs.

South Africa's economy is primarily based on its ability to produce natural resources, such as precious metals and stones, including platinum, gold, and diamonds. However, exploring the hydrocarbon potential of sedimentary basins within the country is projected to diversify the country's economic base. Compared to other countries, minimal exploration and research have been conducted in sedimentary basins offshore of the South African coast. Most hydrocarbon exploration and production in South Africa has been concentrated on the Outeniqua Basin, which is located offshore of the southern coast. Total Exploration and Production Company announced a significant gas condensate discovery within the Outeniqua Basin in February 2019 (Feder, 2019). This discovery has opened up the southern offshore basins in South Africa for renewed exploration. This study used core data from three wells in the Bredasdorp Basin located offshore of the south coast of South Africa (Fig. 1) to develop the reservoir zonation.

The Bredasdorp Basin area is roughly 18,000 km², with stratigraphic sequences thicker than 5000 m, and stretches south-eastward from Cape Town to the Agulhas/Falkland fracture zone in the Indian Ocean (Muntingh and Brown, 1993; Wood, 1995). Sedimentary sequences consist of marine shales, lacustrine source rocks, and Cretaceous to Lower Palaeogene clastic reservoirs. With limited exploration over the years, the petroleum system in the Bredasdorp Basin remains poorly understood. More importantly, reservoir rocks within the basin are vital to the hydrocarbon accumulation and have not been studied in detail.

The workflow in this study relies on core porosity and permeability measurements at room temperature conditions. It is important to note that the relationship between permeability and porosity is crucial in our proposed analysis. This approach differs from the earlier method used by Opuwari et al. (2020b) in the western Bredasdorp Basin. Furthermore,

this study is part of an ongoing study to identify flow zones in South Africa's offshore basins, culminating in the development of a petrophysical reservoir zonation scheme.

Previous studies on reservoir FU zonation and rock typing in the South African offshore basins were conducted by Opuwari et al. (2020a), Opuwari et al. (2019), and Opuwari et al. (2020b) in the Orange Basin, Pletmos Basin, and the western Bredasdorp Basin. Despite the Bredasdorp Basin having over 200 exploration, production, and appraisal wells drilled, there is a paucity of literature describing reservoir flow characterisation. Hence, this study aims to address this knowledge gap by providing a solution through the application of a simple conventional but effective reservoir zonation method for the identification of the vertical and lateral extents of the studied reservoir rock. Four broad methods were used: (1) lithofacies identification from sedimentology reports and well logs, (2) permeability anisotropy from the vertical and horizontal core permeability, (3) hydraulic unit (HU) determination methods (Winland r35 pore throat method (PRT) and reservoir quality index (RQI (HFU) method), and (4) the SMLP FU method.

1.1. Geological overview

The basin developed from a syn-rift that started in the Jurassic and has undergone various regional uplift and subsidence phases. The Bredasdorp Basin post-rift sediments have been favourable targets for hydrocarbon since the first oil discovery in 1987. This discovery led to the development of a sequence stratigraphic model that documented post-rift associated facies across the basin (Broad et al., 2006).

The concept of cyclical sequences was adopted to delineate hydrocarbon plays, in which each region has an identified sequence (Petroleum Agency of South Africa, PASA, 2003). Low-stand system tracts are thought to comprise basin floor turbidite fans, channels, and sheets (Broad et al., 2006). According to De Wit and Ransome (1992), a distinctive chronostratigraphic framework has been mapped for the Bredasdorp Basin (Fig. 2), and the youngest unconformity occurred

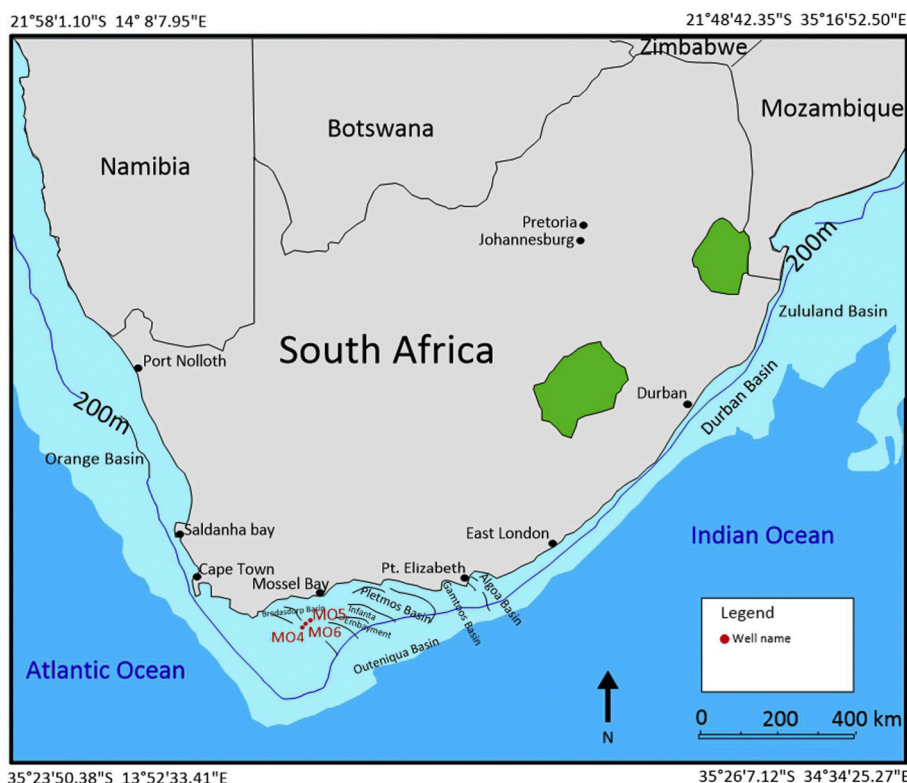


Fig. 1. Location map of study area offshore in South Africa (Petroleum Agency of South Africa 2003).

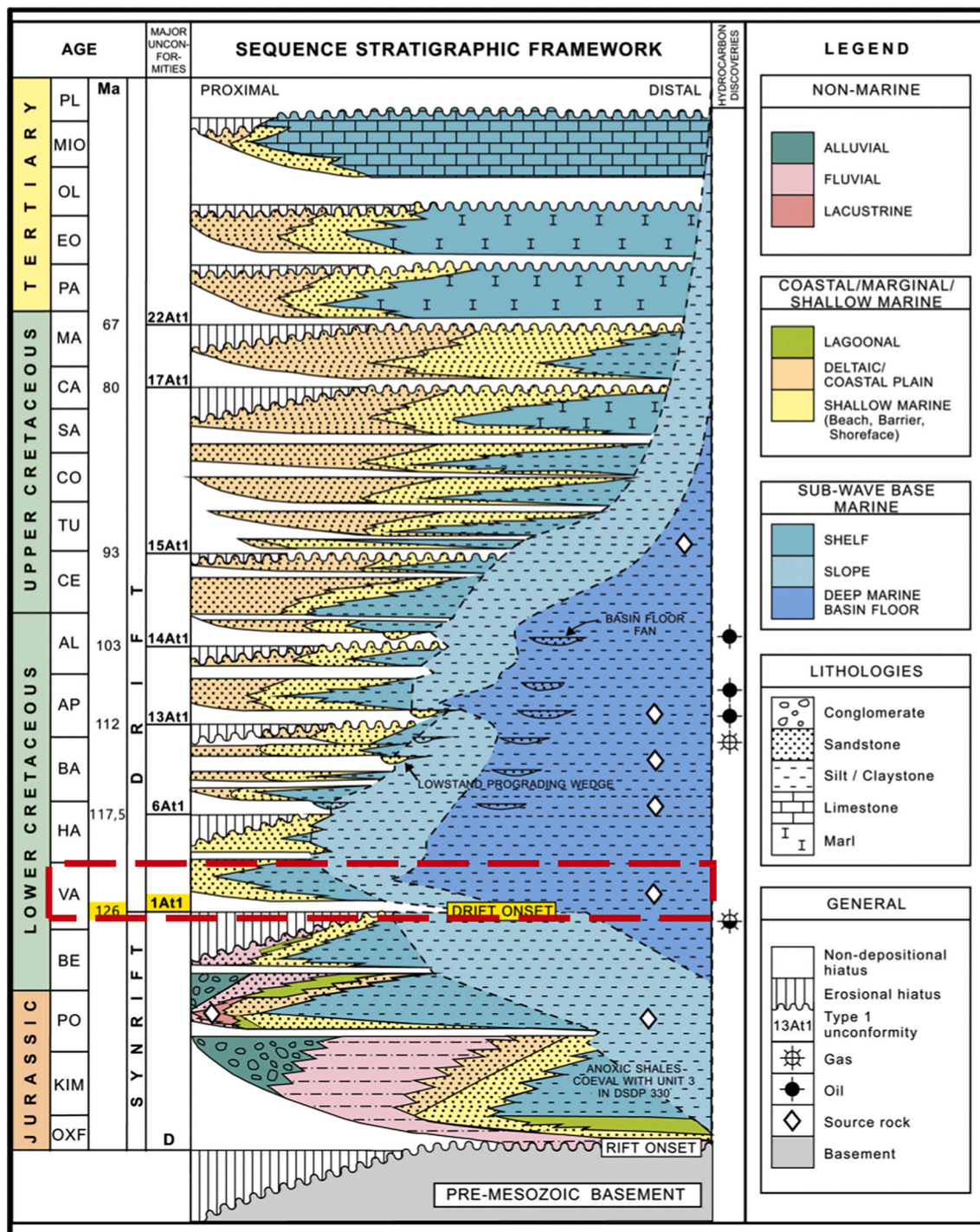


Fig. 2. Chronostratigraphic and sequence chart showing major unconformities as well as possible source rock intervals (Jungslager1999; Ramiah et al., 2019). Red dot rectangle. (For interpretation of the references to colour in this figure legend, the reader is referred to the web version of this article.)

close to the seafloor. The syn-rift and post-rift sequences are separated by the large-scale 1At1 unconformity, which occurred during the late Valanginian period. This study was conducted within the Lower Cretaceous shallow marine sediments highlighted by the red dotted rectangle in Fig. 2.

2. Materials and methods

This study used porosity and permeability data from conventional core analysis of three wells (MO4, MO5, and MO6) from the Bredasdorp Basin offshore of South Africa. The core plug measurements were

performed at room conditions, including the porosity and vertical and horizontal permeability. All samples were thoroughly cleaned under soxhlet extraction using toluene followed by methanol as a solvent, then dried in a vacuum oven at 95 °C until constant weight is attained. The samples were then allowed to cool to room temperature before analysis for gas permeability, Boyle's Law expansion porosity and grain density was performed. The gas permeability was measured using a calibrated steady-state permeameter with dry air as the flowing medium. The flow was allowed to stabilise before readings were taken. The horizontal and vertical plug sample grain volumes were measured using a calibrated helium gas volume expansion meter. The porosimeter used for the

measurement of porosity was checked for any possible leak before analysis was performed.

A total of 501 core plug samples within the sandstone reservoir intervals of the three wells were investigated. A total of 250 plug samples from well MO4, 55 from well MO5, and 196 from well MO6, representing three sandstone reservoir intervals, were obtained. The data analysis process commenced using a Microsoft Excel spreadsheet to perform quality checks and data correction before calculating the petrophysical parameters. A database was created in the Interactive Petrophysics software, and the calculated parameters were loaded for further evaluation.

The workflow began by identifying lithofacies from the integration of sedimentology reports and logs before evaluating petrophysical flow zones. Analyses by two independent analytical flow zone methods, petrophysical rock typing (Winland r35 and FZIs) and FU (SMLP), were adopted to define FUs/zones using core porosity and permeability.

2.1. Petrophysical rock type methods (Winland r35 and Flow Zone Indicator)

2.1.1. Winland r35

Winland (1972) performed measurements on sandstone samples and produced an empirical relationship among the pore-throat size, porosity, and permeability. He established the best match at 35% mercury saturation. Winland's r35 method was published by Kolodzie (1980) to determine the pore-throat radius from core porosity and permeability data (Al-Aruri et al., 1998; Pittman, 1992; Porras and Campos, 2001; Rushing et al., 2008; Xu et al., 2012).

The Winland equation has the following form:

$$\text{Log } r_{35} = 0.732 + 0.588 \log K - 0.864 \log \Phi \quad (1)$$

where r is the pore throat radius (μm), K is the permeability (mD), and Φ is porosity (%).

2.1.2. Flow Zone Indicator

Amaefule et al. (1993) produced a valuable approach to classify reservoirs for RQI calculation, normalised porosity index (NPI), and FZI. Using the methods developed by Amaefule et al. (1993), which have been used successfully by other researchers (Chekani and Kharrat, 2009; El Sharawy and Nabawy, 2019, 2016, 2016; Kadkhodaie-Ilkhchi et al., 2013; Opuwari et al., 2019; Shan et al., 2018; Shenawi et al., 2007; Tavakoli et al., 2011; Tiab and Donaldson, 2015), the studied core samples were classified into HFUs. The RQI, NPI, and FZI parameters were determined using Eqs. 2, 3, and 4 to define the HFUs within the analysed core samples.

$$\text{RQI} = 0.0314 * (\sqrt{\text{Permeability (mD)}/\text{Porosity (v/v)}}) \quad (2)$$

$$\text{NPI} = \text{Porosity}/(1 - \text{Porosity}) \quad (3)$$

$$\text{FZI} = \text{RQI}/\text{NPI} \quad (4)$$

2.1.3. SMLP analysis

SMLP uses storage and flow capacities to determine FUs. Slope variations reflect FUs, while plateaus are interpreted as barriers where negligible to no fluid flow is expected (Gunter et al., 1997; Newsham and Rushing, 2001; Pranter et al., 2004). The SMLP technique was used to identify the possible FUs within the studied core samples. In this method, the analysis was performed per unit foot of core samples using PASA data. The percentage flow capacity (PFC) and percentage storage capacity (PSC) were determined using Eqs. 5 and 6.

$$\text{PFC} = K * h \quad (5)$$

$$\text{PSC} = \Phi * h \quad (6)$$

where h represents the thickness over which the porosity and permeability were determined. SMLP was then constructed by plotting the cumulative PFC versus the cumulative PSC. Paired cumulative PFC and PSC are plotted from minimum to maximum as a function of the depths they represent. Variations in the trend reflect deviations in flow or storage capacity. Steep slopes reflect high speed rates of flow; likewise, horizontal trends indicate negligible or slight flow (Mahjour et al., 2016).

These two approaches were implemented in wells MO4, MO5, and MO6. The results were analysed and compared with the facies to identify the flow zones within the reservoir intervals.

3. Results and discussion

3.1. Lithofacies Identification

Rock type classification of various lithofacies was achieved by integrating sedimentology reports and well logs (gamma ray, resistivity, density, and sonic), which were common to all wells in the study area. The studied well sediments were mainly from shallow marine depositional environments. The sedimentology reports provided detailed core descriptions of the studied wells, which included a rock classification framework based on grain size. Three lithofacies were grouped as lithofacies 1, 2, and 3. Lithofacies 1 is a silty shale and bioturbated sandstone, lithofacies 2 is an interbedded sandstone and shale, with well-sorted very fine sandstone and heavily cemented grains. Conversely, lithofacies 3 is a fine- to medium-grained sandstone with minor shales and moderate cementation (Opuwari et al., 2020b).

A log standardisation process was performed on the gamma ray, resistivity, density, and sonic logs, including environmental corrections, de-spiking, and curve matching before a multi-well histogram plot was generated to establish limits for each identified lithofacies. The well logs were used as input in a cluster analysis model in the Interactive Petrophysics (IP) rock typing module. The rock type cluster analysis results are shown in Table 1 and Fig. 3. The results were integrated with the sedimentology analysis to consolidate the lithofacies rock classification method, which culminated into three rock types as follows:

Lithofacies 1: Silty shale and bioturbated sandstone represent the lowest rock quality (red colour) with an average gamma ray value of 82 api, resistivity of 8 ohmm, density of 2.44 g/cc, and sonic of 73 $\mu\text{s}/\text{ft}$. as shown in (Table 1) and Fig. 3.

Lithofacies 2: Represents fair to moderate reservoir rock (green colour) with an average gamma ray value of 59 api, resistivity of 11.5 ohmm, density of 2.47 g/cc, and sonic of 70 $\mu\text{s}/\text{ft}$. This rock type contains interbedded sandstone and shales, very fine sandstone with well-sorted grains, and is heavily cemented.

Lithofacies 3: Represents moderate to good reservoir rock (blue colour) with an average gamma ray value of 54 api, resistivity of 18 ohmm, density of 2.57 g/cc, and sonic of 67 $\mu\text{s}/\text{ft}$. This rock type contains interbedded sandstone and shales, very fine sandstone with well-sorted grains, and is very well cemented. This lithofacies contains fine- to medium-grained sandstone and is moderately cemented. Lithofacies 3 is ranked as the best reservoir rock, followed by lithofacies 2 and 1.

3.2. Reservoir permeability anisotropy

Understanding the permeability variation is vital for reservoir characterisation. In a homogeneous reservoir, permeability is considered uniform in all directions, whereas in a heterogeneous reservoir, permeability tends to differ with direction. The more heterogeneous a reservoir is, the more variable the permeability (Khalid et al., 2020; Widarsono et al., 2006). The permeability variability in different directions impacts the fluid flow; hence, understanding the effect of permeability anisotropy in a reservoir is crucial. This study presents permeability anisotropy in the vertical and horizontal directions using

Table 1
Well log cluster analysis result for each rock type (lithofacies).

Clusters		GR (api)		Resistivity (ohmm)		Density (g/cc)		Sonic ($\mu\text{s}/\text{ft}$)	
Lithofacies	Points	Mean	*Std.	Mean	*Std.	Mean	*Std.	Mean	*Std.
1	243	82.49	26.31	8.37	2.62	2.44	0.05	73.91	2.10
2	373	59.75	17.58	11.50	5.29	2.47	0.04	70.58	2.42
3	699	54.94	12.22	18.30	5.14	2.57	0.03	67.17	3.59

* Std. = Standard Deviation.

core measured permeability data to express reservoir heterogeneity.

The vertical permeability (K_V) is different from horizontal permeability (K_H) in homogeneous and heterogeneous formations owing to the depositional environment and post-depositional effects. Plotting the distributions of K_H as a function of K_V (Fig. 4) of the wells is a good technique to determine the permeability heterogeneity. A robust relationship was obtained from the cross plot that enabled K_V to be calculated from K_H using the following model:

$$K_V = 1.148 * K_H^{0.695} \quad (R^2 = 0.903) \quad (7)$$

Some samples of well MO4 plotted above the symmetry line, indicating the presence of a subsidiary fracture system (El Sharawy and Nabawy, 2019). The vertical permeability was generally higher than the horizontal permeability in the samples, with a few exceptions. Another approach used in this study to determine the vertical and horizontal reservoir heterogeneity was the permeability anisotropy method. The permeability anisotropy method is the ratio of the horizontal permeability (K_H) to the vertical permeability (K_V) calculated from (El Sharawy and Nabawy, 2019; Nabawy and ElHariri, 2008; Serra, 1983), and is expressed as.

$$\lambda_k = (K_H/K_V)^{0.5} \quad (8)$$

where λ_k is permeability anisotropy (dimensionless).

The calculated permeability anisotropy ranged from 0.04 to 1.26. In the permeability anisotropy classification introduced by El Sharawy and Nabawy (2019), the samples were ranked as moderately anisotropic (0 to 0.5), slightly anisotropic (0.5–1.0), and isotropic (1.0 to 1.1). The difference between the moderate and the slightly anisotropic zones may be related to the pore system's mineralogy and changes (Soleymanzadeh et al., 2019). Plotting the vertical and horizontal permeability as a function of permeability anisotropy (Fig. 4 b and c) showed that the samples were predominantly slightly anisotropic inserted between the moderately anisotropic samples to the left and isotropic samples to the right. The difference between the vertical and horizontal permeability values was evident in the moderately anisotropy zone, with vertical permeability higher than horizontal permeability.

3.3. Petrophysical rock type

3.3.1. Winland r35

The reservoir intervals were subdivided into five FUs/zones based on the calculated pore throat radii from the core porosity and permeability (Table 2). The calculated average r35 value (PRT) was used to identify intervals (flow zones) of similar pore-throat radii and discriminated between flow zones. The Winland r35 method performs very well in primary interparticle, intergranular, and intercrystalline pore systems. However, the presence of fractures or connected vugs causes the Winland method to overestimate r35 values (Jordan et al., 1985; Martin et al., 1997). In this study, flow zones were directly delineated based on the Winland r35 method because of the absence of fractures and vugs in the samples used.

The data plotted on the permeability versus porosity cross plot were superimposed on standard Winland r35 overlay lines (Fig. 5) to characterise rock quality using Winland r35. The plot revealed five different types of flow zones identified as petrophysical rock types (PRTs)

grouped as follows:

PRT1: Megaoporous rock (pore throat radius $\geq 10 \mu\text{m}$).

PRT2: Macroporous rock (pore throat radius between 4.0 and 10 μm).

PRT3: Mesoporous rock (pore throat radius ranging from 2 to 4 μm).

PRT 4: Microporous rock (pore throat radius ranging from 1 to 2 μm).

PRT 5: Nanoporous rock (pore throat radius $\leq 1 \mu\text{m}$).

Points plotted along the same lines represented rocks with similar r35 values and thus had equal rock quality. By interpolation, the r35 value for PRT1 was higher than 10 μm and clustered at the upper part of Fig. 5 with good permeability values. Consequently, it was interpreted as the best rock type and PRT5 with pore throat radius $< 1.0 \mu\text{m}$ was interpreted as the lowest quality rock. The rock quality generally decreased from the upper part, dominated by relatively good permeability values, towards the lower left part of the graph. It is evident from the plot that high porosity alone does not necessarily correlate to good rock quality; instead, permeability correlates better with good rock quality and flow.

Dividing the wells into FUs/zones using the calculated average r35 values was possible by assessing significant changes within the reservoir that depicted changes in pore throat radius reflecting different FUs. This approach delineated the studied wells and generated four distinct FUs/zones, as presented in Table 2.

3.3.2. FZI

The computation of FZI parameters from core porosity and permeability data using the modified grouping (Nabawy and Al-Azazi, 2015) resulted in five distinct HFUs, as presented in Table 2. The log–log plot of RQI versus NPI using FZI classification yielded five different HFUs with some overlapping (Fig. 6a).

Samples with similar calculated FZI values fell on a similar line with a similar gradient value. In contrast, samples with different FZI values appeared on separate lines. Five unique parallel lines were indicated by distinct HFUs. The flow properties deteriorated from HFU1 to HFU5 as the FZI values decreased. HFU1 had the best rock-type property with an FZI $> 5 \mu\text{m}$. On the contrary, HFU 5 had the lowest rock-type property exhibiting FZI values $< 1 \mu\text{m}$ with an average porosity of $< 5.0\%$ and permeability $< 1 \text{ mD}$, and was classified as an impervious rock.

The RQI is plotted with permeability and porosity (Fig. 6b and c) to establish a relationship and determine which variables contribute more to flow. It is evident from the plots that permeability (Fig. 6c) contributes more to flow, showing a better relationship with RQI than porosity. The FZI is plotted as a function of porosity and permeability to obtain a relationship and enable prediction (Fig. 8a and b). In both cases of RQI and FZI against porosity and permeability, it was observed that permeability related better with RQI and FZI, which indicates that permeability is more influenced by the pore throat radius connectivity than the pore volume and that permeability contributes significantly to the reservoir quality. Our interpretation agrees with previous studies of FZI in sandstone and carbonate reservoirs (Li et al., 2017; Opuwari et al., 2019; Shan et al., 2018; Teh et al., 2012).

3.4. SMLP FU

The SMLP method plots the cumulative flow capacity (kh) against the cumulative storage capacity (Φh). Paired permeability with interval

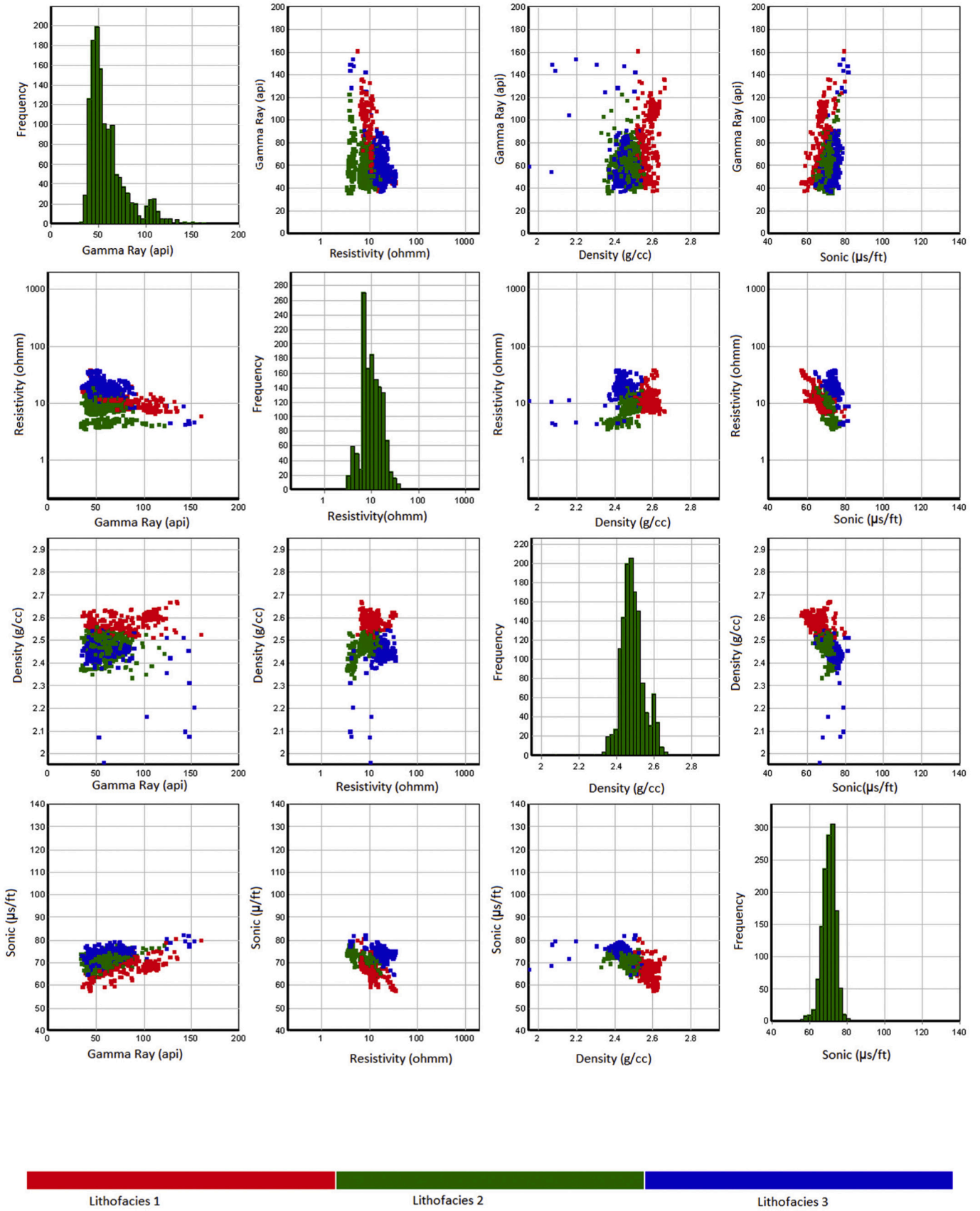


Fig. 3. The rock type cluster analysis results for well showing lithofacies.

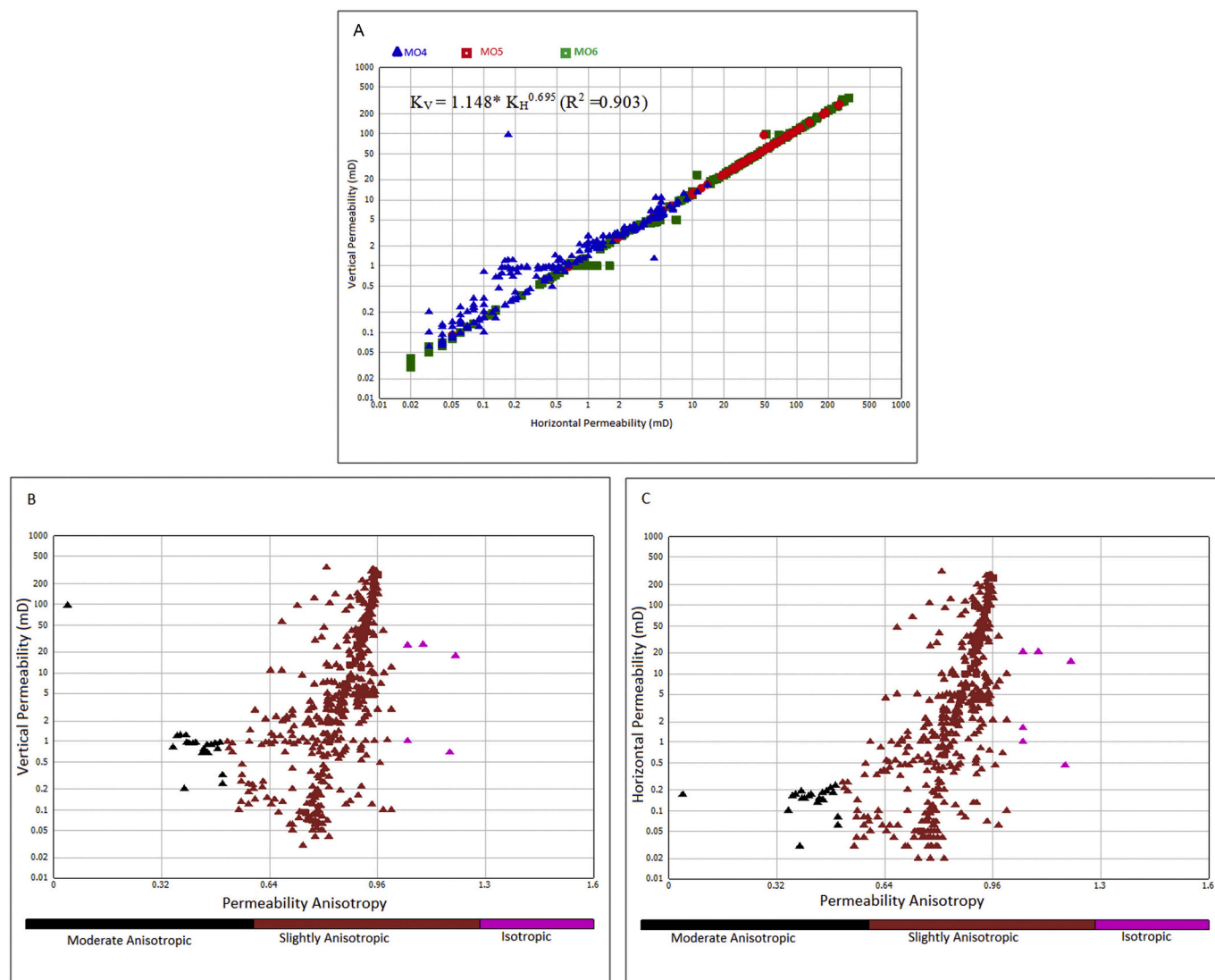


Fig. 4. (a) Plotting the distributions of KH as a function of KV to determine the permeability. (b) Vertical permeability as a function of permeability anisotropy (c) horizontal permeability as a function of anisotropy.

thickness and porosity with interval thickness values were first established, normalised, and then the cumulative values were established and plotted (Grier and Marshall, 1992). The SMLP approach was adopted to determine the extent of permeability variation and indicate the part of the reservoir interval contributing to flow (Gunter et al., 1997) (Mahjour et al., 2016). The trend along the 45° angle on the storage capacity line, which was relatively constant, indicated that the storage capacity was relatively distributed in that interval. Parts with high slopes have a higher flow capacity percentage than storage capacity; therefore, they have higher reservoir speeds, and are known as fast (reservoir) zones. The parts of the curve with a lower slope and more of a plateau have a low flow capacity and are known as tight zones (Chopra et al., 1987; Newsham and Rushing, 2001; Pranter et al., 2004).

In this study, FUs (speed zone, baffle, and barrier/tight) were interpreted by selecting slope variations or inflexion points. The trend that plots below 45° mainly represents the baffle and barrier/tight units, while the trend that plots above 45° contains the preferential flow zone. Using the SMLP method, the main FUs/zones are illustrated in their appropriate stratigraphic positions. Based on the SMLP plot results (Figs. 7–9), the reservoir intervals in each well were divided into three types of zones/units (speed zone, baffle zone, and seal unit).

Seven FUs were identified for well MO4, FU1, FU2, FU3, FU4, FU5,

FU6, and FU7 (Fig. 7). The best FU in well MO4 was FU7 because its trend was close to 45°, indicating 36% flow capacity and 21% storage capacity, and was interpreted as a baffle unit. The other baffle units identified were FU3, FU4, and FU5, collectively contributing to 53% flow capacity and 51% storage capacity. FUs 1, 2, and 6 were baffle/tight units with negligible flow capacity but possessed a storage capacity of 28%. Seven FUs were represented in well MO5 (Fig. 8), of which FU5 and 6 were the high flow zones, and contributed 60% of the flow capacity and 54% of the storage capacity. FUs 1, 2, 4, and 7 were baffle units that contributed 40% of the flow capacity and 38% of the storage capacity. FU3 was a barrier unit with negligible flow but represented 8% of the storage capacity. Five FUs were identified in well MO6 (Fig. 9). FUs 2 and 4 were the high-speed zones, which contributed 62% of the flow capacity and 21% of the storage capacity. Baffle FUs were 5, 6, and 7, and collectively contributed 38% of the flow capacity and 42% of the storage capacity. FUs 1, 3, and 8 were the barriers with negligible contribution to flow, but had a storage capacity of 37%.

4. Reservoir zonation

A comparison of the various flow zonation methods in the studied wells indicates that each FU encompasses a wide range of lithofacies,

Table 2

Results of calculated Hydraulic Units from the Winland's r35 and Hydraulic Flow Unit methods for the division of rock types into different categories modified after Nabawy et al. (2018) and Opuwari et al. 2020. Where PRT is Petrophysical Rock Type; r35 is calculated pore throat radius, and FZI is Flow Zone Indicator. The values of r35 are used to group the rock into different rock types (PRT 1 -5) while FZI is used for the ranking of rocks.

Well	Top Depth (m)	Bottom Depth (m)	Thickness (m)	Porosity %	Permeability mD	Zone/ Unit	r35 (µm)	PRT	Rock Type	FZI (µm)	Ranking
				15–20	100–500	High	>10	1	Megaporous	5–10	Very Good
				10–15	20–100	Moderate	4–10	2	Macroporous	3–5	Good
				5–10	5–20	Low	2–4	3	Mesoporous	2–3	Fair
				5–10	1–5	Very Low	1–2	4	Microporous	1–2	Poor
				<5	<1.0	Tight	<1	5	Nanoporous	<1	Impervious
MO4	2620.7	2632.3	11.6	8.3	0.2	Tight	0.4	5	Nanoporous	0.7	Impervious
	2632.3	2650.1	17.8	7.1	0.1	Tight	0.2	5	Nanoporous	0.4	Impervious
	2650.1	2675.7	25.6	10.0	0.5	Tight	0.6	5	Nanoporous	0.7	Impervious
	2675.7	2680.7	5.0	9.2	0.2	Tight	0.3	5	Nanoporous	0.5	Impervious
	2680.7	2717.4	36.7	12.9	2.4	Very Low	1.1	4	Microporous	1.2	Poor
MO5	2573.7	2576.5	2.8	12.8	4.5	Very Low	2.1	4	Microporous	2.0	Fair
	2576.5	2581.7	5.2	14.0	37.2	Moderate	6.1	2	Macroporous	3.9	Good
	2581.7	2586.6	4.9	14.3	19.7	Low	3.7	3	Mesoporous	2.5	Fair
	2586.6	2590.6	4.0	13.7	30.7	Moderate	5.8	2	Macroporous	3.8	Good
MO6	2562.1	2576.6	14.5	11.9	3.2	Very Low	2.5	4	Microporous	1.9	Poor
	2576.6	2600.4	23.8	12.9	43.8	Moderate	7.0	2	Macroporous	4.9	Good
	2600.4	2611.7	11.3	11.4	2.2	Very Low	1.9	4	Microporous	1.7	Poor
	2611.7	2625.2	13.5	12.5	8.2	Low	2.6	3	Mesoporous	2.5	Fair
	2625.2	2645.4	20.2	6.7	0.2	Tight	0.6	5	Nanoporous	0.9	Impervious

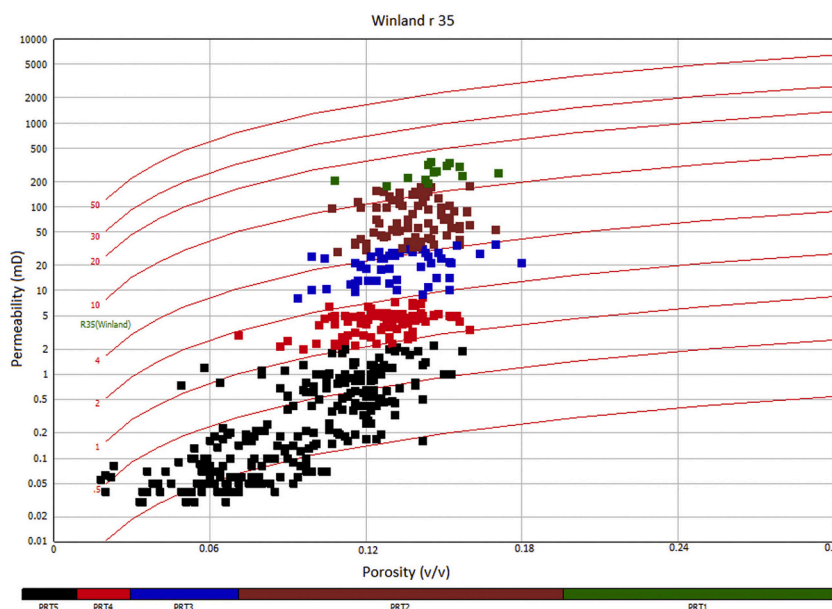


Fig. 5. The Plot of Permeability against Porosity with Winland r35 pore throat radius for identification of rock types.

porosity, and permeability values. A combination of the two different methods (PRT and FZI) makes assigning the wells into FUs possible by evaluating significant changes in PRT and FZI, reflecting a change in connectivity and FU. The average values of PRT and FZI are used to identify the flow zone that leads to a comprehensive interpretation of flow zones throughout the wells, using the criteria established in Table 2. The two methods used for flow zone delineation showed good agreement with minor inconsistencies due to differences in scale. The edited curve data module on the IP software that defined the curve types created within the IP were used to develop lithology/lithofacies in conjunction with the gamma ray log. Additionally, the fill data gap module that allows the production of continuous data from discrete datasets, such as routine core analysis plug data, was also used to generate continuous porosity, permeability, permeability anisotropy, Winland r35, FZI, and storage and flow capacity logs as illustrated in Figs. 10–12. The results of the reservoir zonation methods revealed four flow zones delineated as tight, very-low, low, and moderate zones.

The reservoir zonation results for well MO4 divided the studied reservoir into two main zones (tight and very-low zones), as shown in Fig. 10. The tight zone was predominantly composed of lithofacies 1, characterised by low reservoir quality parameters (porosity <10%, permeability <0.5 mD, pore throat radius < 0.6 µm, and FZI ≤ 0.7 µm). This zone was characterised by a moderate to slightly anisotropic (0.035 to 0.9) pore architecture. The tight zone rock quality was related to the nanoporous rock type (PRT5), which was ranked as an impervious reservoir quality in well MO4. This tight flow zone with a collective thickness of 60 m, retained a storage potential of 38% (track 10) but had a flow potential of <5% (track 11), as shown in Fig. 10. However, the reservoir quality tended to improve slightly towards the base from depths of 2680 m to 2717 m, which was delineated as a very-low flow zone. This very-low flow zone comprises lithofacies 2, an interbedded sandstone and shale, with very fine sandstone with well-sorted grains, which are heavily cemented. This flow zone was characterised by poor reservoir quality parameters (average porosity of 12.9%, permeability of

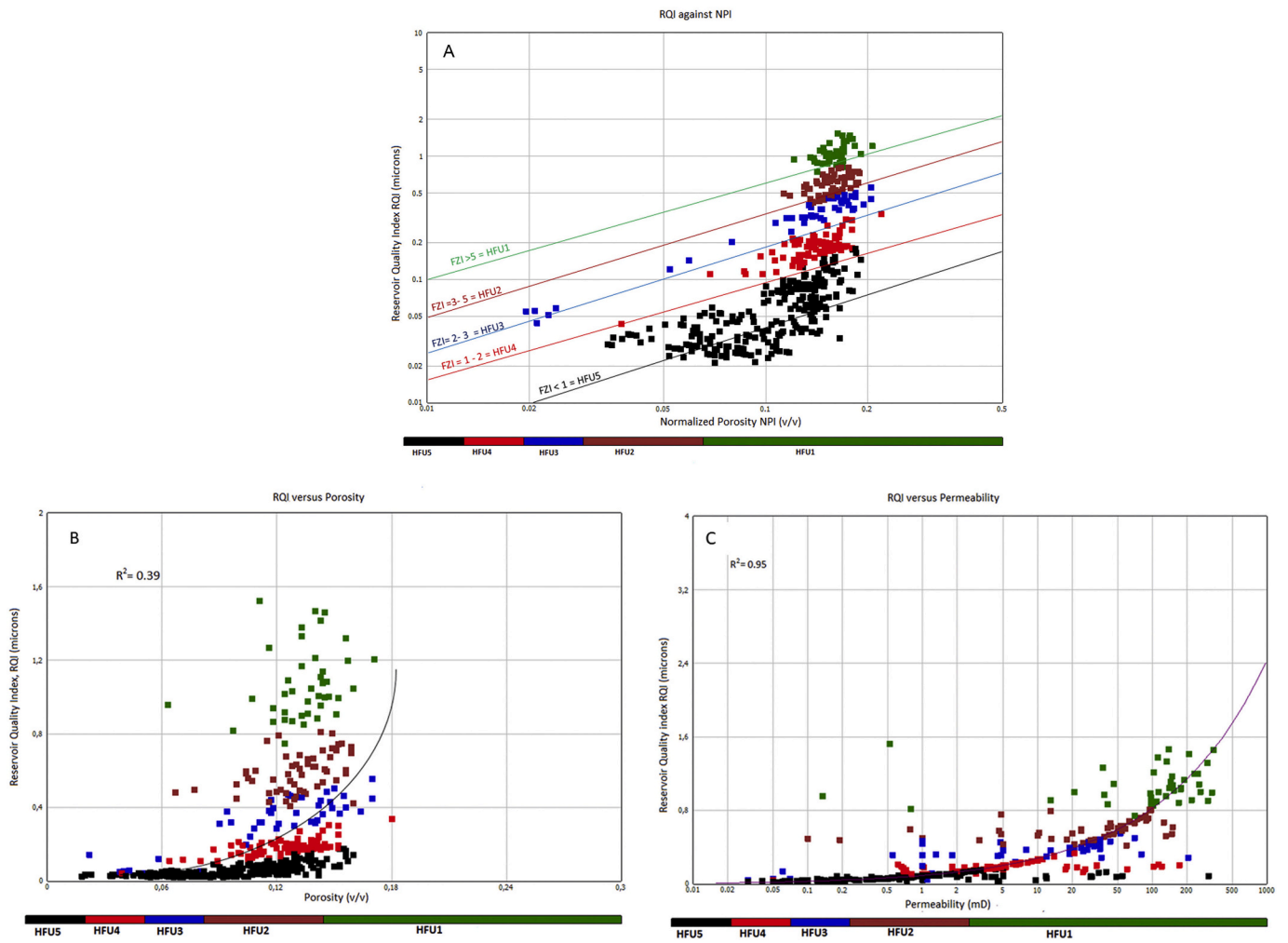


Fig. 6. a. Log-log plot of RQI vs. NPI for FZI, showing five different rock classifications. b. RQI versus Porosity. c. RQI against Permeability.

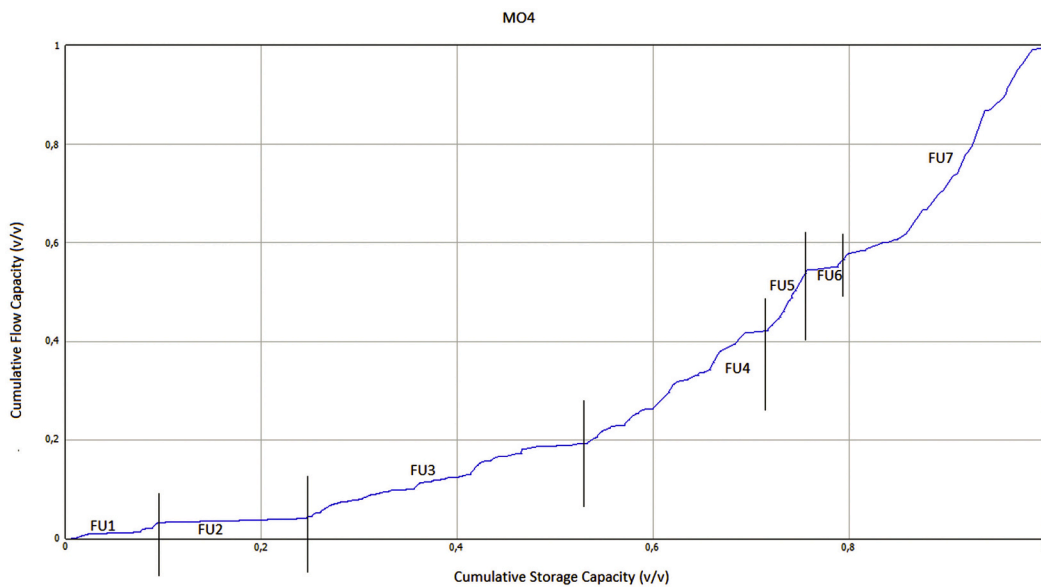


Fig. 7. Cross-plot of cumulative storage capacity vs cumulative flow capacity for well MO4.

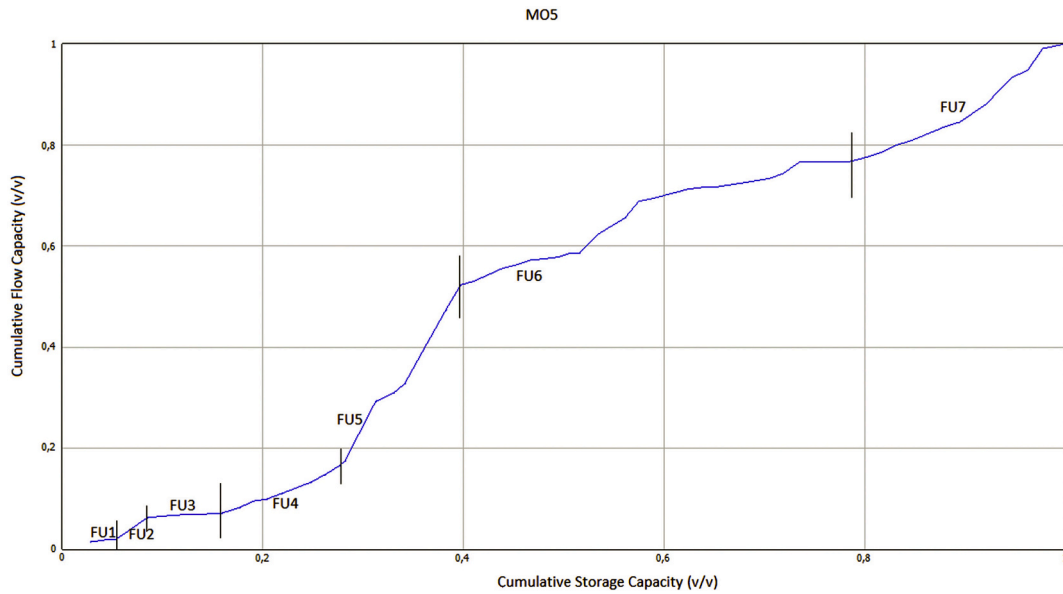


Fig. 8. Cross-plot of cumulative storage capacity vs cumulative flow capacity for well MO5.

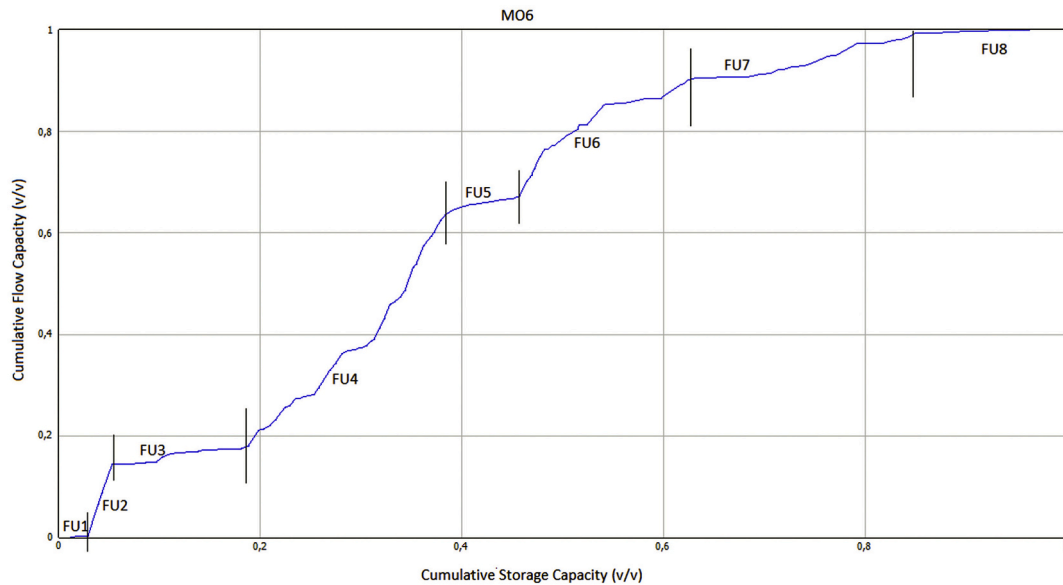


Fig. 9. Cross-plot of cumulative storage capacity vs cumulative flow capacity for well MO6.

2.4 mD, pore throat radius of 1.1 μm , and FZI of 1.2 μm), and was ranked as a poor rock type. A relatively slightly higher anisotropic (0.45–0.97) pore architecture with an average permeability anisotropy of 0.81 (slightly anisotropic), was recorded in this very-low flow zone. An increase in storage and flow capacities within the very-low flow zone represents the best reservoir rock type for well MO4. This thick (36.7 m) very-low flow zone is interpreted as the most favourable zone for gas production, which comprises FU7 (Fig. 7). The shale content in the reservoir unit tends to decrease with depth with a corresponding increase in sandstone, which may be attributed to the relatively better reservoir quality observed at the reservoir base, which is the very-low flow zone.

Four flow zones (very low, two moderate, and one low) composed of intercalated shale and sandstone (lithofacies 1, 2, and 3) within the zones are represented in well MO5 (Fig. 11). The very-low flow zone has lithofacies 2 at the top and lithofacies 1 at the base with an average porosity of 12.8%, a permeability of 4.5 mD, a pore throat radius of 2.1

μm , and an FZI of 2.0 μm . The upper part of this zone shows better reservoir quality, whereas the lower part has a lower reservoir quality. Slight anisotropy (0.74–0.94), with an average value of 0.87, was recorded in this zone. Underlying the very-low flow zone is a moderate flow zone predominantly composed of fine- to medium-grained sandstone and moderately cemented rock (lithofacies 3). This zone is characterised by moderate reservoir quality parameters (average porosity, 14.0%; permeability, 37.2 mD; pore throat radius, 6.1 μm ; and FZI, 3.9 μm). An average value of 0.91 permeability anisotropy was recorded for this zone. This moderate zone is predominantly the macroporous rock type (PRT2) and is ranked as good (HFU2) reservoir rock composed of FU5 and FU6 and is interpreted as having a high flow capacity (Fig. 8).

Below the moderate zone is a low-flow zone with lithofacies 1 at the top and lithofacies 2 at the base. The average porosity of 14.3%, a permeability of 19.7 mD, pore throat radius of 4 μm (PRT3), and FZI of 2.7 μm (HFU3) ranked as a fair reservoir rock quality. Slight anisotropy (0.84–0.94) with an average of 0.9 pore architecture characterises this

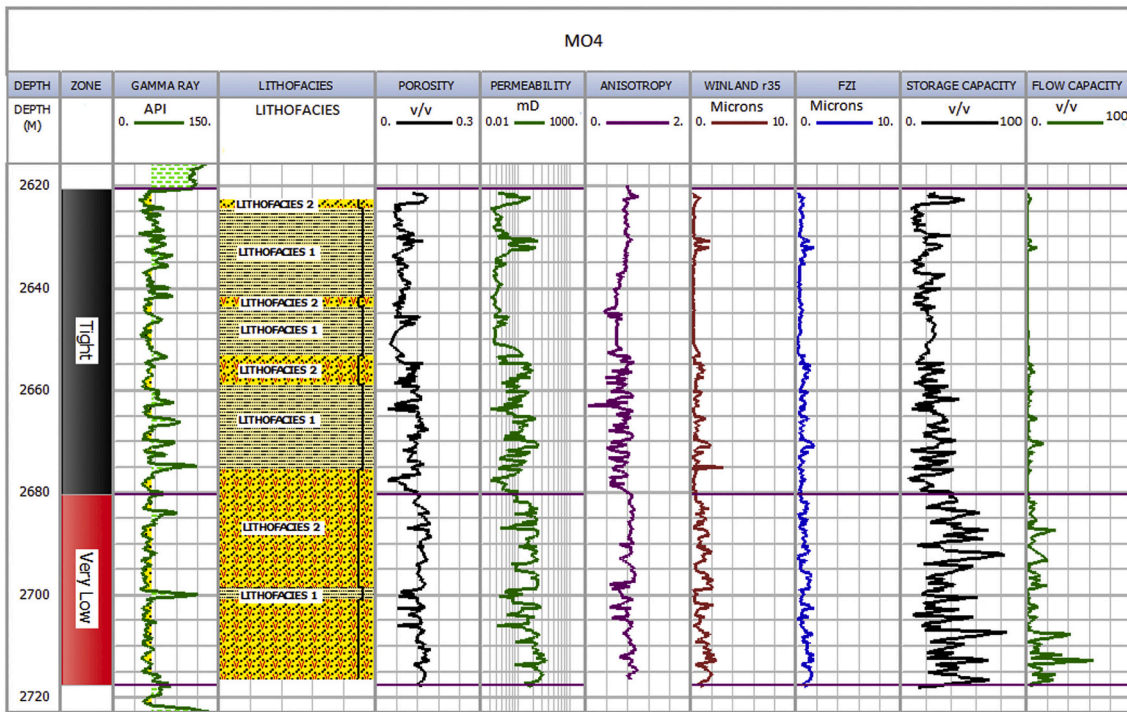


Fig. 10. Integrated results for well MO4 showing Zones in track 2, Gamma Ray log in track 3, Porosity in track 4, Permeability in track 5, Permeability Anisotropy in track 6, Winland r35 in track 7, FZI in track 8, Storage Capacity in track 9, and Flow Capacity in track 10.

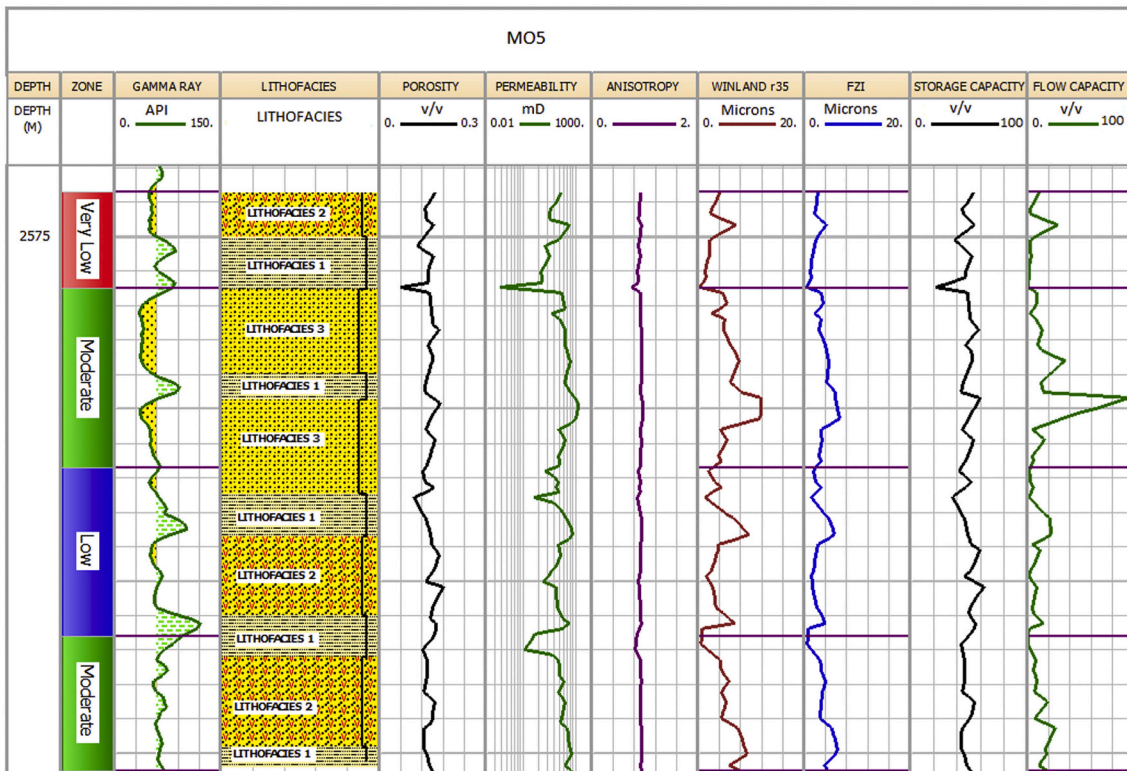


Fig. 11. Integrated results for well MO5 showing Zones in track 2, Gamma Ray log in track 3, Porosity in track 4, Permeability in track 5, Permeability Anisotropy in track 6, Winland r35 in track 7, FZI in track 8, Storage Capacity in track 9, and Flow Capacity in track 10.

zone. The base of this zone, which contains lithofacies 2, demonstrates a better reservoir quality. The moderate zone below the low-flow zone is predominantly composed of lithofacies 2 and is slightly anisotropic

(0.91). An average porosity of 13.7%, permeability of 30.7 mD, pore throat radius of 5.8 μm (PRT2), and FZI of 3.8 μm (good reservoir rock) was recorded in this zone. This zone also contained FU6 and FU7, with a

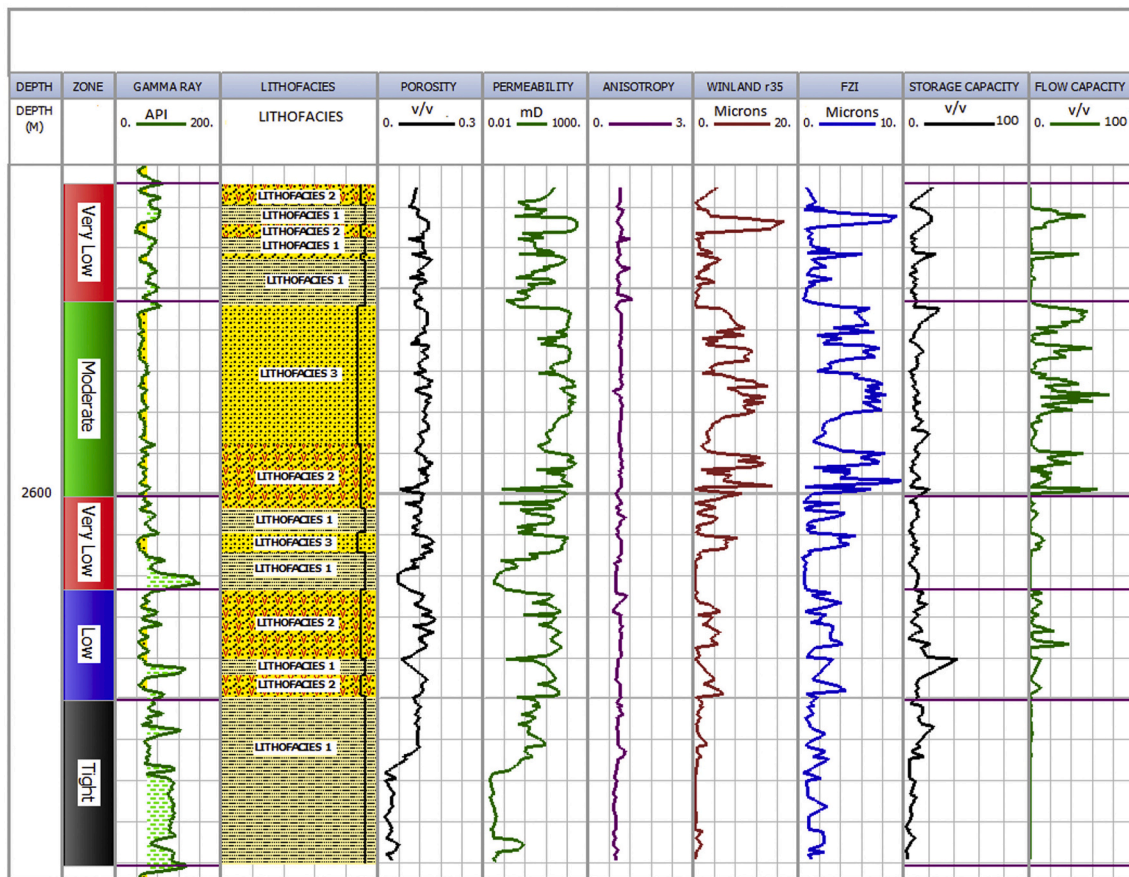


Fig. 12. Integrated results for well MO6 showing Zones in track 2, Gamma Ray log in track 3, Porosity in track 4, Permeability in track 5, Permeability Anisotropy in track.

high flow capacity (Fig. 8). It was observed that the upper-moderate zone is the best reservoir zone displaying good petrophysical parameters, characterised by higher storage and flow capacity (tracks 8 and 9). Generally, a higher value of the average anisotropic value is recorded as the quality of the reservoir rock increases from very-low (0.87), low (0.9), to moderate (0.91) flow zones.

Five flow zones (two very low, one moderate, one low, and one tight) composed of intercalated shale and sandstone within the zones, except for the moderate zone, are found in well MO6 (Fig. 12). The upper very-low zone is composed of intercalated lithofacies 1 and 2 with an average porosity of 11.9%, a permeability of 3.2 mD, pore throat radius of 2.5 μm (PRT4), and FZI of 1.9 μm (low rock quality). An average anisotropy value of 0.87 was recorded for this zone. A cumulative flow and storage capacity of 18% were recorded in this zone. Underlying this very-low zone is a moderate flow zone with lithofacies 3 at the top and lithofacies 2 at the base with an average porosity of 12.9%, a permeability of 44 mD, pore throat radius of 7.0 μm (macroporous rock type), and FZI of 4.9 μm (good reservoir rock). This moderate flow zone with an average anisotropic value of 0.91, is the best flow zone delineated for well MO6 and for the studied wells because of its thickness (23.8 m) and reservoir qualities compared to the other moderate zones of well MO5. The flow speed capacity of 45% (Fig. 9) and storage capacity of 20% (FU4) of this moderate zone are higher than in any other flow zone and consequently, it is regarded as the best flow zone identified.

Underlying the moderate zone is the second very-low zone composed of lithofacies 1 and lithofacies 3, characterised by an average porosity of 11.4%, permeability of 2.2 mD, anisotropy of 0.86, pore throat radius of 1.9 μm (microporous rock), and FZI of 1.7 μm (poor rock type). A low flow zone is shown below the very-low flow zone predominantly composed of lithofacies 2 with an average porosity of 12.5%,

permeability of 8 mD, pore throat radius of 2.6 μm (mesoporous rock), and FZI 2.5 μm (fair rock quality). The low flow zone also displayed fair to good storage and flow potential (tracks 10 and 11). Below the low flow zone is a tight zone composed chiefly of lithofacies 1 (track 3), characterised by an average porosity of 6.7%, permeability of 0.2 mD, anisotropy of 0.81, pore throat radius of 0.6 μm (nanoporous rock), and FZI of 0.9 μm (impervious rock), which is regarded as the most reduced rock quality in well MO6.

In general, lithofacies do not always correspond to petrophysical flow zones. The studied rock is predominantly slightly anisotropic. The tight zones exhibit fluid storage potential (an average porosity of 6.7 to 10%) but have no flow capacity (permeability ≤ 0.5 mD). The very-low zone parameters are interpreted to be used as the cut-off to discriminate between productive and non-productive zones (tight). The best flow zone (moderate) is in the middle of the reservoir. The second moderate flow zone identified in well MO5 is comparable to the moderate zones in MO2 and MO3. The low flow zone in well MO5 is also comparable to the low flow zone of well MO1 in the Western Bredasdorp Basin (Opuwari et al., 2020b). These similar zones are traceable.

5. Conclusion

This study aims to investigate and establish whether the flow zones identified in the western Bredasdorp Basin extend to the eastern region and identify new flow zones in the north-western Bredasdorp Basin. Three lithofacies were grouped as lithofacies 1, 2, and 3. Lithofacies 1 is a silty shale and bioturbated sandstone, lithofacies 2 is an interbedded sandstone and shale, with very fine sandstone with well-sorted grains, and very well cemented. Conversely, lithofacies 3 is a fine- to medium-grained sandstone with minor shale and is moderately cemented.

Lithofacies 3 is ranked as the best reservoir rock, followed by lithofacies 2 and 1.

The studied wells were divided into five PRTs (PRT 1–5) and five HFUs (HFU 1–5) that culminated in the reservoir zonation into four flow zones (moderate, low, very low, and tight). The moderate flow zone of well MO6 exhibits the best reservoir quality. The moderate flow zone is 23.8 m thick with a sand to shale ratio of 98% characterised by moderate reservoir quality parameters (an average porosity of 12.9%, permeability of 52 mD, pore throat radius of 6.5 μm (macroporous rock type), and FZI of 3.9 μm (good reservoir rock). This zone also has a speed flow capacity of 42% (FU4) and a storage capacity of 21%. In general, lithofacies do not always correspond to the petrophysical flow zones. The studied rock is predominantly slightly anisotropic.

The tight zones showed fluid storage potential (an average porosity of 6.7 to 10%) but had no flow capacity (permeability ≤ 0.5 mD). The very-low flow zone parameters are interpreted to be used as the cut-off to discriminate between productive and non-productive zones (tight flow zone). The low-flow zone could serve as a conduit for fluid transfer between zones. The best flow zone (moderate) is in the middle of the reservoir. The second moderate zone identified in well MO5 is comparable to the moderate zones in MO2 and MO3, and the low flow zone in well MO5 is also comparable to the low flow zone of well MO1 in the Western Bredasdorp Basin. These similar zones are traceable. Mineralogy analyses and production measurements are recommended to understand the minerals and their nature present in each flow zone and establish whether the flow zones are in communication or isolated.

Declaration of Competing Interest

The authors declare that no known competing financial interests or personal relationships could have influenced the work reported in this paper.

Acknowledgements

The authors express thanks to the Petroleum Agency of South Africa (PASA) for providing the data used in this work. The Senergy Company is also acknowledged for providing the IP software package.

References

Al-Aruri, A., Ali, F.B., Ahmad, H.A., Samad, S.A., 1998. Rock Type and Permeability Prediction from Mercury Injection Data: Application to a Heterogeneous Carbonate Oil Reservoir, Offshore Abu Dhabi (United Arab Emirates), in: Abu Dhabi International Petroleum Exhibition and Conference. Society of Petroleum Engineers.

Al-Jawad, S.N., Saleh, A.H., 2020. Flow units and rock type for reservoir characterization in carbonate reservoir: case study, south of Iraq. *Journal of Petroleum Exploration and Production Technology* 10, 1–20.

Amaefule, J.O., Altunbay, M., Tiab, D., Kersey, D.G., Keelan, D.K., 1993. Enhanced Reservoir Description: Using Core and Log Data to Identify Hydraulic (Flow) Units and Predict Permeability in Uncored Intervals/Wells, in: SPE Annual Technical Conference and Exhibition. Society of Petroleum Engineers.

Broad, D.S., Jungslager, E.H.A., McLachlan, I.R., Roux, J., 2006. Offshore Mesozoic Basins. *The Geology of South Africa. Geological Society of South Africa*, 553. Johannesburg/Council for Geoscience, Pretoria, p. 571.

Carman, P.C., 1937. Fluid flow through granular beds. *Trans. Inst. Chem. Eng.* 15, 150–166.

Chekani, M., Kharrat, R., 2009. Reservoir rock typing in a carbonate reservoir-cooperation of core and log data: case study. In: SPE/EAGE Reservoir Characterization & Simulation Conference. European Association of Geoscientists & Engineers (p. cp-170).

De Wit, M.J., Ransome, I.G., 1992. Inversion Tectonics of the Cape Fold Belt, Karoo and Cretaceous Basins of Southern Africa: Proceedings of the Conference on Inversion Tectonics of the Cape Fold Belt, Cape Town, South Africa, 2–6 December 1991. Taylor & Francis.

Ebanks, W.J., 1987. Flow unit concept-integrated approach to reservoir description for engineering projects. AAPG 71. United States.

El Sharawy, M.S., Nabawy, B.S., 2016. Geological and Petrophysical Characterization of the lower Senonian Matulla Formation in Southern and Central Gulf of Suez, Egypt. *Arab. J. Sci. Eng.* 41, 281–300. <https://doi.org/10.1007/s13369-015-1806-7>.

El Sharawy, M.S., Nabawy, B.S., 2019. Integration of electrofacies and hydraulic flow units to delineate reservoir quality in uncored reservoirs: A case study, Nubia Sandstone Reservoir, Gulf of Suez, Egypt. *Nat. Resour. Res.* 28, 1587–1608.

Feder, J., 2019. Offshore: making a Comeback after the Downturn. *J. Pet. Technol.* 71, 27–31.

Gomes, J.S., Ribeiro, M.T., Strohmenger, C.J., Naghban, S., Kalam, M.Z., 2008. Carbonate Reservoir Rock Typing-the Link between Geology and SCAL, in: Abu Dhabi International Petroleum Exhibition and Conference. Society of Petroleum Engineers.

Grier, S.P., Marschall, D.M., 1992. Reservoir Quality: Part 6. Geological Methods.

Gunter, G.W., Finneran, J.M., Hartmann, D.J., Miller, J.D., 1997. Early determination of reservoir flow units using an integrated petrophysical method. In: SPE Annual Technical Conference and Exhibition. Society of Petroleum Engineers.

Hearn, C.L., Ebanks, W.J., Tye, R.S., Ranganathan, V., 1984. Geological factors influencing reservoir performance of the Hartzog Draw Field, Wyoming. *J. Pet. Technol.* 36, 1–335.

Jordan, C.F., Connolly, T.C., Vest, H.A., 1985. Middle Cretaceous carbonates of the Mishrif formation, Fateh field, offshore Dubai, UAE. In: *Carbonate Petroleum Reservoirs*. Springer, pp. 425–442.

Kadkhodaie-Ilkhchi, R., Rezaee, R., Moussavi-Harami, R., Kadkhodaie-Ilkhchi, A., 2013. Analysis of the reservoir electrofacies in the framework of hydraulic flow units in the Whicher Range Field, Perth Basin, Western Australia. *J. Pet. Sci. Eng.* 111, 106–120.

Kassab, M.A., Teama, M.A., Cheadle, B.A., El-Din, E.S., Mohamed, I.F., Mesbah, M.A., 2015. Reservoir characterization of the lower Abu Madi Formation using core analysis data: El-Wastani gas field, Egypt. *J. Afr. Earth Sci.* 110, 116–130.

Khadem, B., Saber, M.R., Eslahati, M., Arbab, B., 2020. Integration of rock physics and seismic inversion for rock typing and flow unit analysis: A case study. *Geophys. Prospect.* 68, 1613–1632.

Khalid, P., Akhtar, S., Khurram, S., 2020. Reservoir Characterization and Multiscale Heterogeneity Analysis of Cretaceous Reservoir in Punjab Platform of Middle Indus Basin, Pakistan. *Arabian Journal for Science and Engineering* 1–20.

Kolodzie, S., 1980. Analysis of pore throat size and use of the Waxman-Smiths equation to determine OOIP in Spindle Field, Colorado. In: SPE Annual Technical Conference and Exhibition. Society of Petroleum Engineers.

Li, J., Yu, T., Liang, X., Zhang, P., Chen, C., Zhang, J., 2017. Insights on the gas permeability change in porous shale. *Advances in Geo-Energy Research* 1, 69–73.

Mahjour, S.K., Al-Askari, M.K.G., Masih, M., 2016. Identification of flow units using methods of Testerman statistical zonation, flow zone index, and cluster analysis in Tabnaq gas field. *Journal of Petroleum Exploration and Production Technology* 6, 577–592.

Martin, A.J.J., Solomon, S.T., Hartmann, D.J., 1997. Characterization of petrophysical flow units in carbonate reservoirs. *AAPG Bull.* 81, 734–759.

Muntingh, A., Brown, L.F., 1993. Sequence Stratigraphy of Petroleum Plays, Post-Rift Cretaceous Rocks (Lower Aptian to Upper Maastrichtian), Orange Basin, Western Offshore, South Africa: Chapter 4: Recent Applications of Siliciclastic Sequence Stratigraphy.

Nabawy, B.S., Al-Azazi, N.A., 2015. Reservoir zonation and discrimination using the routine core analyses data: the upper Jurassic Sab'atayn sandstones as a case study, Sab'atayn basin, Yemen. *Arab. J. Geosci.* 8, 5511–5530.

Nabawy, B.S., Barakat, M.K., 2017. Formation evaluation using conventional and special core analyses: Belayim Formation as a case study, Gulf of Suez, Egypt. *Arab. J. Geosci.* 10, 25.

Nabawy, B.S., ElHariri, T.Y., 2008. Electric fabric of cretaceous clastic rocks in Abu Gharadig basin, Western Desert, Egypt. *J. Afr. Earth Sci.* 52, 55–61.

Nabawy, B.S., Basal, A.M.K., Sarhan, M.A., Safa, M.G., 2018. Reservoir zonation, rock typing and compartmentalization of the Tortonian-Serravallian sequence, Tamsah Gas Field, offshore Nile Delta, Egypt. *Mar. Pet. Geol.* 92, 609–631.

Newsham, K.E., Rushing, J.A., 2001. An integrated work-flow model to characterize unconventional gas resources: Part I-Geological Assessment and Petrophysical Evaluation. In: SPE Annual Technical Conference and Exhibition. Society of Petroleum Engineers.

Opuwari, M., 2010. Petrophysical evaluation of the Albian age gas bearing sandstone reservoirs of the O-M field, Orange basin, South Africa. University of the Western Cape, Bellville South Africa (PhD Thesis).

Opuwari, M., Kaushalendra, B.T., Momoh, A., 2019. Sandstone reservoir zonation using conventional core data: A case study of lower cretaceous sandstones, Orange Basin, South Africa. *J. Afr. Earth Sci.* 153, 54–66.

Opuwari, M., Amponsah-Dacosta, M., Mohammed, S., Egesi, N., 2020a. Delineation of sandstone reservoirs of Pletmos Basin offshore South Africa into Flow units using Core Data. *S. Afr. J. Geol.* 2020 (123), 479–492.

Opuwari, M., Mimonitu, Mohammed, S., Ile, C., 2020b. Determination of Reservoir Flow Units from Core Data: A Case Study of the Lower Cretaceous Sandstone Reservoirs, Western Bredasdorp Basin Offshore in South Africa. *Natural Resources Research*, pp. 1–20.

Petroleum Agency, S.A., 2003. South African Exploration Opportunities. Information Brochure. South African Agency for Promotion of Petroleum.

Pittman, E.D., 1992. Relationship of porosity and permeability to various parameters derived from mercury injection-capillary pressure curves for sandstone. *AAPG Bull.* 76, 191–198.

Porras, J.C., Campos, O., 2001. Rock typing: A key Approach for Petrophysical characterization and definition of flow Units, Santa Barbara field, Eastern Venezuela Basin. In: SPE Latin American and Caribbean Petroleum Engineering Conference. Society of Petroleum Engineers.

Pranter, M.J., Hurlley, N.F., Davis, T.L., 2004. Sequence-Stratigraphic, Petrophysical, and Multicomponent Seismic Analysis of a Shelf-Margin Reservoir: San Andres Formation (Permian), Vacuum Field, New Mexico, United States.

Ramiah, K., Trivedi, K.B., Opuwari, M., 2019. A 2D geomechanical model of an offshore gas field in the Bredasdorp Basin, South Africa. *Journal of Petroleum Exploration and Production Technology* 9, 207–222.

- Rushing, J.A., Newsham, K.E., Blasingame, T.A., 2008. Rock typing: Keys to understanding productivity in tight gas sands. In: SPE Unconventional Reservoirs Conference. Society of Petroleum Engineers.
- Serra, O.E., 1983. Fundamentals of Well-Log Interpretation.
- Shalaby, M.R., 2021. Petrophysical characteristics and hydraulic flow units of reservoir rocks: Case study from the Khatatba Formation, Qasr field, North Western Desert, Egypt. *J. Pet. Sci. Eng.* 198, 108143.
- Shan, L., Cao, L., Guo, B., 2018. Identification of flow units using the joint of WT and LSSVM based on FZI in a heterogeneous carbonate reservoir. *J. Pet. Sci. Eng.* 161, 219–230.
- Shenawi, S.H., White, J.P., Elrafie, E.A., El-Kilany, K.A., 2007. Permeability and water saturation distribution by lithologic facies and hydraulic units: a reservoir simulation case study. In: SPE Middle East Oil and Gas Show and Conference. Society of Petroleum Engineers.
- Slatt, R.M., Hopkins, G.L., 1990. Scaling geologic reservoir description to engineering needs. *J. Pet. Technol.* 42, 202–210.
- Soleymanzadeh, A., Parvin, S., Kord, S., 2019. Effect of overburden pressure on determination of reservoir rock types using RQI/FZI, FZI* and Winland methods in carbonate rocks. *Pet. Sci.* 16, 1403–1416.
- Tavakoli, V., Rahimpour-Bonab, H., Esrafil-Dizaji, B., 2011. Diagenetic controlled reservoir quality of south Pars gas field, an integrated approach. *Compt. Rendus Geosci.* 343, 55–71.
- Teh, W., Willhite, G.P., Doveton, J.H., 2012. Improved reservoir characterization in the Ogallah field using petrophysical classifiers within electrofacies. In: SPE Improved Oil Recovery Symposium. Society of Petroleum Engineers.
- Tiab, D., Donaldson, E.C., 2015. Petrophysics: Theory and Practice of Measuring Reservoir Rock and Fluid Transport Properties. Gulf Professional Publishing.
- Widarsono, B., Jaya, I., Muladi, A., 2006. Permeability vertical-to-horizontal anisotropy in Indonesian oil and gas reservoirs: a general review. In: International Oil Conference and Exhibition in Mexico. Society of Petroleum Engineers.
- Winland, H., 1972. Oil accumulation in response to pore size charges, Weyburn field. Saskatchewan. Amoco Production Company Research Department F72–G25. Google Scholar.
- Wood, M., 1995. Development potential seen in Bredasdorp basin off South Africa. *Oil Gas J.* 93.
- Xu, C., Heidari, Z., Torres-Verdin, C., 2012. Rock classification in carbonate reservoirs based on static and dynamic petrophysical properties estimated from conventional well logs. In: SPE Annual Technical Conference and Exhibition. Society of Petroleum Engineers.